Edinburgh Research Explorer

FGF signaling controls somite boundary position and regulates segmentation clock control of spatiotemporal Hox gene activation

Link:
[Link to publication record in Edinburgh Research Explorer](#)

Document Version:
Publisher's PDF, also known as Version of record

Published In:
Cell

FGF Signaling Controls Somite Boundary Position and Regulates Segmentation Clock Control of Spatiotemporal *Hox* Gene Activation

Julien Dubrulle, Michael J. McGrew,
and Olivier Pourquié[1]
Laboratoire de génétique et de physiologie
  du développement (LGPD)
Developmental Biology Institute of Marseille (IBDM)
CNRS–INSERM–Université de la méditerranée–AP
  de Marseille
Campus de Luminy, Case 907
13288 Marseille Cedex 09
France

Summary

Vertebrate segmentation requires a molecular oscillator, the segmentation clock, acting in presomitic mesoderm (PSM) cells to set the pace at which segmental boundaries are laid down. However, the signals that position each boundary remain unclear. Here, we report that FGF8 which is expressed in the posterior PSM, generates a moving wavefront at which level both segment boundary position and axial identity become determined. Furthermore, by manipulating boundary position in the chick embryo, we show that *Hox* gene expression is maintained in the appropriately numbered somite rather than at an absolute axial position. These results implicate FGF8 in ensuring tight coordination of the segmentation process and spatiotemporal *Hox* gene activation.

Introduction

In a vertebrate embryo, the most overt metameric structures are the somites which give rise to the segmented structures of the body including the axial skeleton, the dermis of the back and all skeletal muscles (Hirsinger et al., 2000). These epithelial spheres of paraxial mesoderm are formed by groups of cells that repeatedly bud off from the rostral end of the mesenchymal presomitic mesoderm (PSM), on either side of the neural tube. New mesenchymal cells enter the caudal PSM, as a consequence of continuing posterior gastrulation, maintaining the length of this tissue during axis extension. The PSM is not a homogeneous tissue. In the chick embryo, it can be subdivided into a posterior region about two-thirds of its length in which cells are organized as a loose mesenchyme, and an anterior region in which the epithelialization process has begun (Duband et al., 1987). The expression domains of many genes expressed in the PSM are limited to either one or the other of these two regions such as *paraxis* and *pax3* for the anterior region and *FGF8* and *Brachyury* for the posterior region (Burgess et al., 1995; Crossley and Martin, 1995; Goulding et al., 1994; Knezevic et al., 1997).

The first overt sign of segmentation is seen in the striped expression pattern of several genes in the anterior region of the PSM. The establishment of these segmental patterns of expression is thought to result from an earlier specification event occurring more caudally in the PSM in response to intrinsic cues (Keynes and Stern, 1988). The precise mechanism by which PSM cells become allocated to segments is currently unknown.

Many attempts to alter the segmentation program of the PSM either by grafting it in various ectopic locations or by ablating different regions of this tissue have been reported. In all these experiments, the original segmentation schedule of the PSM was not modified, suggesting that the timing of segment boundary formation is an autonomous property of PSM cells (Aoyama and Asamoto, 1988; Deuchar and Burgess, 1967; Menkes and Sandor, 1977; Packard, 1978; Palmeirim et al., 1998). We refer to this committed state of PSM cells with respect to their segmentation schedule as segmental determination. Similarly, the axial identity of the paraxial mesoderm appears to be established very early in the PSM. PSM from a given regional level transplanted to a different level in a host embryo retains its original identity (Kieny et al., 1972). In operated embryos, the combinatorial expression of *Hox* genes characteristic of the original axial level of the transplant is not modified in the grafted PSM (Nowicki and Burke, 2000). Therefore, cells located in the PSM are usually considered to be pre-endowed with a determined segmentation schedule and a defined axial identity.

This intrinsic property of the PSM to segment formed the basis of a series of models which proposed that the periodicity of vertebrate segment formation is driven by an internal oscillator or clock. These models include the "clock and wavefront" model, Meinhardt's model, the "cell cycle" model, and the "clock and trail" model (Cooke and Zeeman, 1976; Kerszberg and Wolpert, 2000; Meinhardt, 1986; Stern et al., 1988). Molecular evidence for the existence of a clock has been obtained on the basis of the periodic expression in the PSM of several genes related to Notch signaling (Pourquié, 2000). The segmentation clock is thought to play a role in the periodic activation of Notch signaling in the PSM which results in formation of the regular array of somitic boundaries. How the temporal periodicity of the clock oscillations is translated into the periodic array of segmental boundaries remains unknown.

In this paper, we demonstrate that cells of the caudal region of the PSM are labile with respect to their segmentation schedule. Segmental determination occurs at the level of a determination front whose position along the anteroposterior axis in the PSM is controlled by FGF8. Overexpressing FGF8 in the paraxial mesoderm by in ovo electroporation blocks segment formation by maintaining the caudal PSM identity of cells in regions which should normally form somites. Displacing the position of the determination front by altering FGF signaling leads to a shift of the position of somitic boundaries indicating that their positioning is controlled by FGF8. Finally, we show that by slowing the posterior progres-

[1] Correspondence: pourquie@ibdm.univ-mrs.fr

sion of the wavefront, FGF8 treatment can increase the number of clock oscillations experienced by PSM cells without altering their absolute axial position in this tissue. Cells which experience an extra oscillation become incorporated into a differently numbered somite and exhibit *Hox* expression indicative of a more posterior fate when compared with contralateral control cells. Therefore, *Hox* expression remains appropriate to the somitic number rather than to the original axial level of the somitic cells. Thus, our data indicate a coupling between the segmentation clock and the *Hox*-dependent axial patterning system.

Results and Discussion

Caudal PSM Cells Are Labile with Respect to Their Segmentation Program

We undertook a precise analysis of when the segmentation boundaries of PSM cells become determined. To do this, we performed anteroposterior (AP) inversions of somite-length regions of the PSM, in 12- to 16-somite stage chick embryos (Figure 1A). The effect of the manipulation on segmental organization was evaluated after a reincubation of 3 to 24 hr by examining the formed somite boundaries. Since establishment of the segmental pattern is tightly associated with the formation of the prospective anterior and posterior somitic compartments, we also examined the expression of the Notch ligand *delta1*, whose expression is restricted to the caudal somite half.

In the rostral PSM, the forming caudal boundary of somite 0 and somite −I is morphologically visible so that the precise delimitation of the region to be inverted is possible. When the orientation of somite 0 or somite −I was reversed, a somite exhibiting boundaries properly positioned and a perfectly reversed polarity formed (n = 8/8; Figure 1B). Thus, this region is fully determined in regard to segmentation. Inversion of somite-length fragments in the region from somites −II to −IV resulted in the formation of ectopic boundaries and in an abnormal anteroposterior subdivision in the graft (n = 18/27; Figure 1C). Therefore, this region is not labile with respect to its segmentation program. In contrast, inversion of somite-length fragments in the region from somite −V to somite −XII led to a normal segmentation pattern, demonstrating a lack of determination for the caudal two-thirds of the PSM (Figure 1D; n = 19/20). This data demonstrate that segmental determination takes place in the PSM around the level of somite −IV. Because this position is not fixed, but regresses along the AP axis as somitogenesis proceeds, we term this PSM level the determination front. The determination front corresponds approximately to the zone of sensitivity to heat shock (Stern et al., 1988).

FGF8 Maintains the Caudal Identity of the PSM

We examined the expression patterns of potential candidate genes which might play a role in segmental determination in the PSM. One candidate, FGF8, is a well-characterized signaling molecule whose mRNA is expressed in the caudal PSM (Crossley and Martin, 1995). It is expressed in a graded fashion extending from the primitive streak/tail bud to the level of the determination front,

at the interface of the caudal undetermined and the rostral determined region (Figures 1E–1H). Of the four receptors for this molecule, only *FGFR1* is expressed in the PSM, and it exhibits a peak of expression encompassing the determination front (Figure 1I; Patstone et al., 1993). Given their strong gastrulation phenotype resulting in an almost complete absence of paraxial mesoderm, neither *FGF8* nor *FGFR1* null mutants in the mouse are informative with respect to the segmentation process (Sun et al., 1999; Yamaguchi et al., 1994). However, a small proportion of *FGFR1* mutants form paraxial mesoderm which does not segment into somites suggesting that this receptor is implicated in somitogenesis (Yamaguchi et al., 1992). Therefore, FGF8 and FGFR1 are attractive candidates for playing a role in the control of segmental determination of the caudal PSM cells.

To test whether FGF8 plays a role in the control of segmental determination of PSM cells, we developed an in ovo electroporation technique to misexpress DNA constructs in the PSM of 10- to 20-somite stage chick embryos. Primitive streak stage embryos were coelectroporated with an FGF8 and a GFP expression vector while control embryos were electroporated with GFP alone. Overexpressing chick FGF8b strongly perturbed somitogenesis as seen by the formation of smaller somites or the complete absence of somites in GFP expressing regions (n = 50/62) (Figures 2A–2F). Parasagittal sections of such electroporated embryos demonstrate that cells that should have normally formed repeated epithelial somites retained a uniform mesenchymal aspect (Figures 2G and 2H). Expression of *Brachyury*, which is normally restricted to the caudal PSM, was strongly upregulated and the expression domain was expanded anteriorly (n = 6/6, Figures 2I–2L). In contrast, *pax3*, which is expressed rostral to the determination front, was downregulated in the domain of FGF8 overexpression (n = 4/4, Figures 2M and 2N). We also examined the expression of *MyoD*, which is expressed in a segmental fashion in myotomal derivatives. *MyoD* was not detected in the region of FGF8 overexpression, suggesting that differentiation of paraxial mesoderm derivatives was also prevented in the PSM (n = 6/7, Figures 2O and 2P). In contrast, GFP overexpression alone had no effect on somitogenesis or on expression of these different marker genes (n = 35/39, Figures 2C, 2D, 2G, 2I, and 2J). Altogether, these results indicate that FGF8 is sufficient to maintain the caudal identity of PSM cells and suggest that downregulation of FGF signaling at the level of the determination front is required for PSM cells to proceed further with their segmentation program.

Grafting FGF8 Beads Leads to Smaller Somite Formation

To further address the role of FGF8 in segmentation, we grafted a heparin-acrylic bead soaked in FGF8b between the PSM and the lateral mesoderm of 10- to 20-somite stage embryos (Figure 3A). We reasoned that while the gradient of endogenous *FGF8* becomes progressively displaced caudally during tail-bud extension, the bead will remain at a constant axial level, and thus the operation will locally alter the putative FGF8 concentration gradient in the adjacent PSM. The effect of FGF8
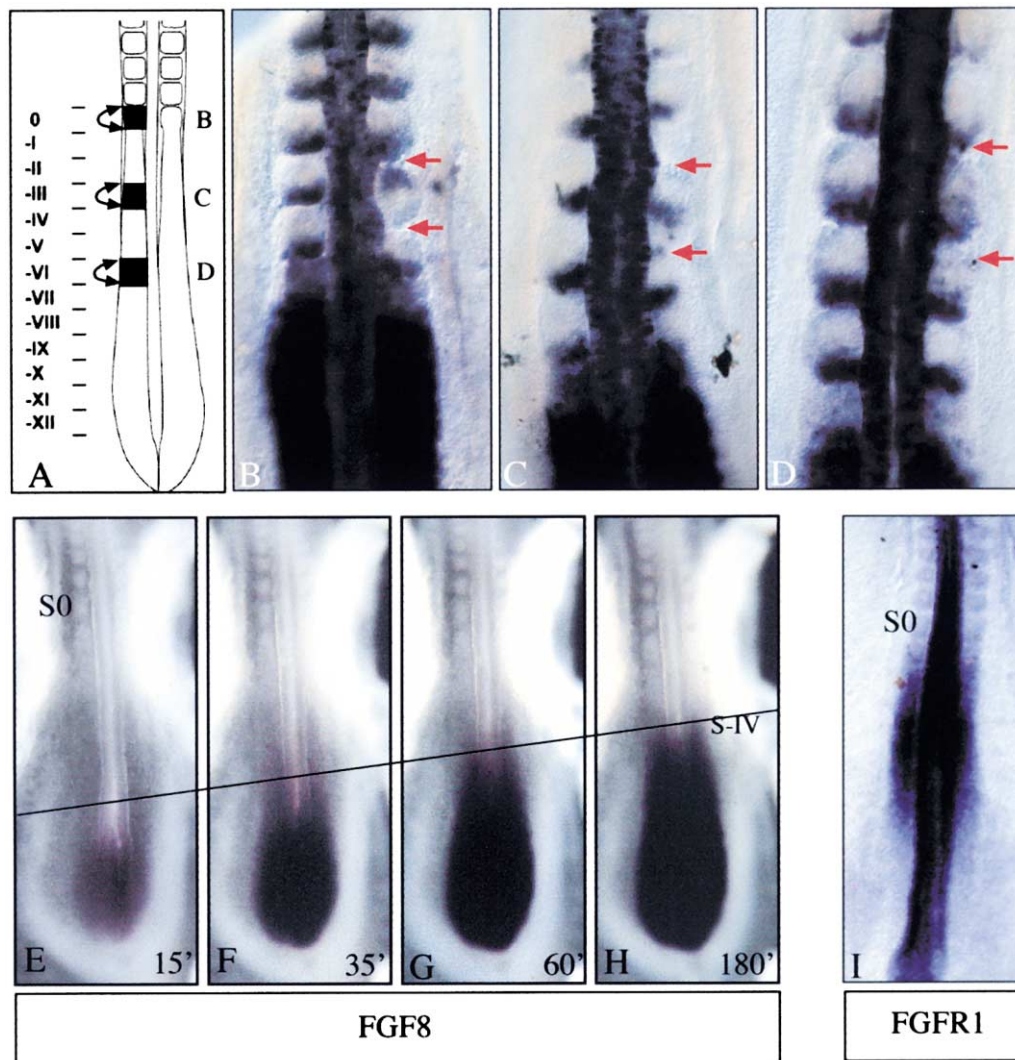
Figure 1. The Caudal PSM Region Is Undetermined with Respect to Segmentation and Expresses FGF8 in a Graded Fashion

Results of inversions of PSM fragments of one somite in length from the level of S0 to S−XII as illustrated in (A). Formation of morphological somitic boundaries and anteroposterior patterning of the somitic compartments in the inverted tissue were evaluated after in situ hybridization with the *c-delta1* probe. The inverted PSM fragment is delimited by red arrows. (B) HH stage 12 embryo operated at the level of S0 hybridized with *c-delta1*. (C) HH stage 12 embryo operated at the level of S−III hybridized with *c-delta1*. (D) HH stage 13 embryo operated at the level of S−VI hybridized with *c-delta1*. (E-H) A 19-somite stage embryo hybridized with *FGF8* and photographed after 15 (E), 35 (F), 60 (G), and 180 min (H) of staining reaction to demonstrate the graded expression of this mRNA in the caudal PSM. (I) In situ hybridization with the *FGFR1* probe of a 14-somite stage embryo. (B–I) Dorsal view. Rostral is to the top. Red arrows delimit the extent of the inversion.

beads on segmentation was examined after 18–24 hr of incubation, when the region adjacent to the bead had formed somites. In embryos grafted with beads soaked in FGF8, somites appeared smaller on the operated side, becoming offset from those on the control side over a region which could extend up to 6–7 somites rostral to the bead (n = 27/33, Figures 3B, 4A, and 4B). Thus, the bead acts on cells located close to the level of the determination front at the time of bead implantation (Figure 3A) where the peak of *FGFR1* expression is seen (Figure 1I). Caudally to the grafted bead, a larger somite formed and thereafter a normal segmental pattern was observed (Figure 3B). In this manner, the total number of somites was the same in the operated and control sides. Implantation of the beads within the PSM resulted

in a stronger effect similar to that seen in electroporated embryos. In this case the operation led to an absence of somitic boundary formation immediately rostral to the bead over a distance of up to three somites whereas up to three smaller somites form rostral to this zone (not shown).

When the bead was placed midway between the caudal-most PSM and S-IV, only the part of the PSM which was located between the bead and the somite −IV was affected (Figures 3C and 3D, n = 6/7). Cells located caudal to the bead never form small somites even though they are competent to do so if FGF8 were provided to them from a caudal source. No effect on segmentation was ever detected in cells which were rostral to the somite −IV at the time of surgery, even when
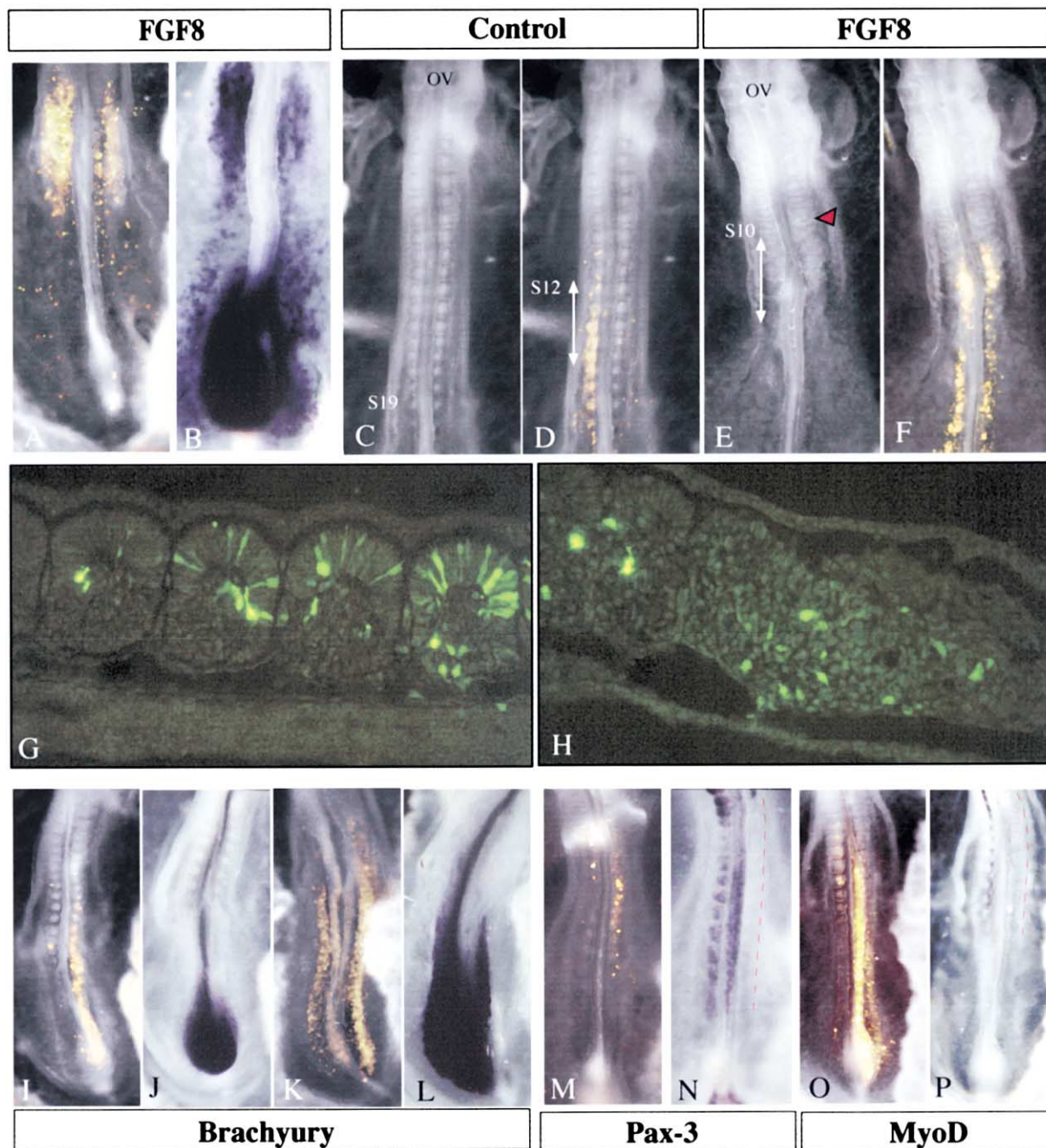
Figure 2. Overexpression of FGF8 Abolishes Somitogenesis and Maintains the Caudal Identity of PSM Cells

(A and B) Embryo coelectroporated with FGF8 and GFP expression vectors. (A) GFP expression (in yellow). (B) Whole-mount in situ hybridization of the embryo with *FGF8* reveals ectopic *FGF8* expression domains corresponding to the GFP-positive areas in the somitic region and in the lateral plate.

(C and D) 19-somite embryo electroporated with a GFP expression plasmid alone. (C) Bright-field showing normal somitogenesis. (D) GFP expression.

(E and F) Coelectroporation of GFP with an FGF8 expression vector leads to an absence of somites. Embryo shown in (E) and (F) was incubated for the same time period as that shown in (C) and (D). The rostral region exhibits developmental features such as an almost closed otic vesicle (OV) characteristic of a 19-somite embryo. (E) Bright-field showing that somitogenesis is interrupted at the level of somite 10 (S10). (F) GFP expression. Red arrow indicates the rostral extent of the GFP domain. White double arrows mark the position of the sections shown in (G) and (H). S12: somite 12.

(G) Parasagittal section of the designated region of control embryo in (D) (white arrow) reveals the presence of GFP-positive cells in epithelial somites.

(H) Parasagittal section of the embryo in (E) (white arrow) demonstrates the loss of epithelial somites in the region overexpressing FGF8.

(I and J) Control embryo electroporated with GFP alone. (I) GFP expression. (J) Whole-mount in situ hybridization with *Brachyury*. (K–P) Embryos coelectroporated with GFP and FGF8. (K) GFP expression. (L) Whole-mount in situ hybridization with *Brachyury*.

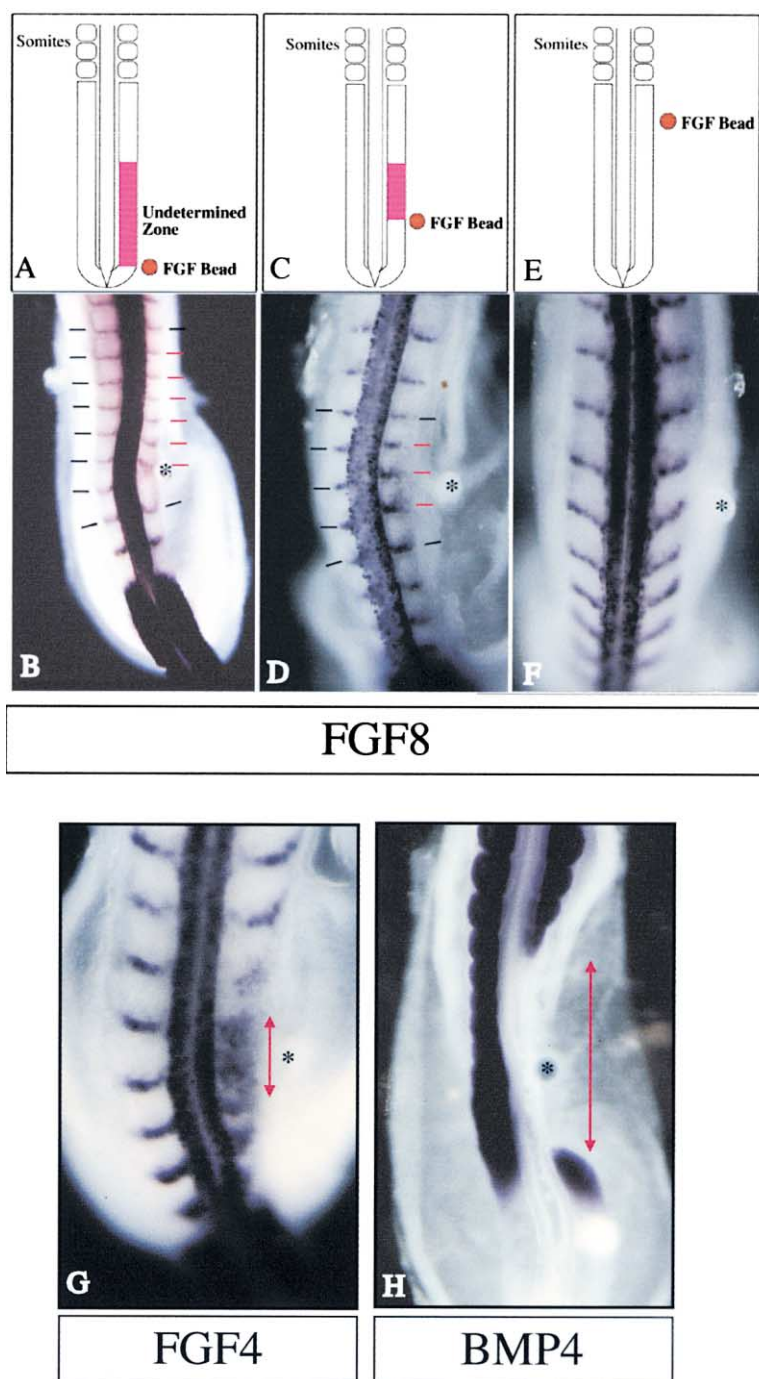(M) GFP expression. (N) Whole-mount in situ hybridization with *pax3*.

Figure 3. Anisotropic Effect of FGF8 on Somite Formation

(A, C, and E) Schematic representation of the graft of the FGF8 bead illustrating the level of the bead graft in the PSM corresponding to the embryos shown in (B), (D), and (F), respectively. (B, D, and F) Whole-mount in situ hybridization with *c-delta1* of grafted HH stage 17 embryos. (A and B) An FGF8 bead was grafted in the caudal-most region of the PSM. (C and D) Graft of an FGF8 bead at the position indicated in (C). (E and F) Graft of an FGF8 bead in the rostral region of the PSM. (G and H) Whole-mount in situ hybridization of HH stage 17 embryos with *c-delta1* after implantation of a FGF4 bead (G) or with *paraxis* after implantation of a BMP4 bead (H), as shown in (A). Asterisks mark the position of the bead and red double arrows in (G) and (H) show the extent of the effect. Dorsal views, anterior to the top.

beads were directly grafted adjacent to this region of the PSM (Figures 3E and 3F, n = 18/20). The fact that rostral PSM exposed to FGF bead grafts does not form smaller somites can seem paradoxical because this region continues to strongly express *FGFR1* (Figure 1I). This can however be explained if one hypothesizes that

a cell's response to FGF signaling changes once it passes the determination front at somite −IV. Thus, only the cells of the caudal PSM located between the bead and the determination front respond to FGF8, indicating an anisotropic effect of this factor on the PSM.

Such an anisotropic effect would be expected in a

(O) GFP expression. (P) Whole-mount in situ hybridization with *MyoD*. The red hatched line marks the lateral extent of the paraxial mesoderm on the electroporated side in (N) and (P).
Dorsal views. Anterior is to the top. In (G) and (H), anterior is to the left.
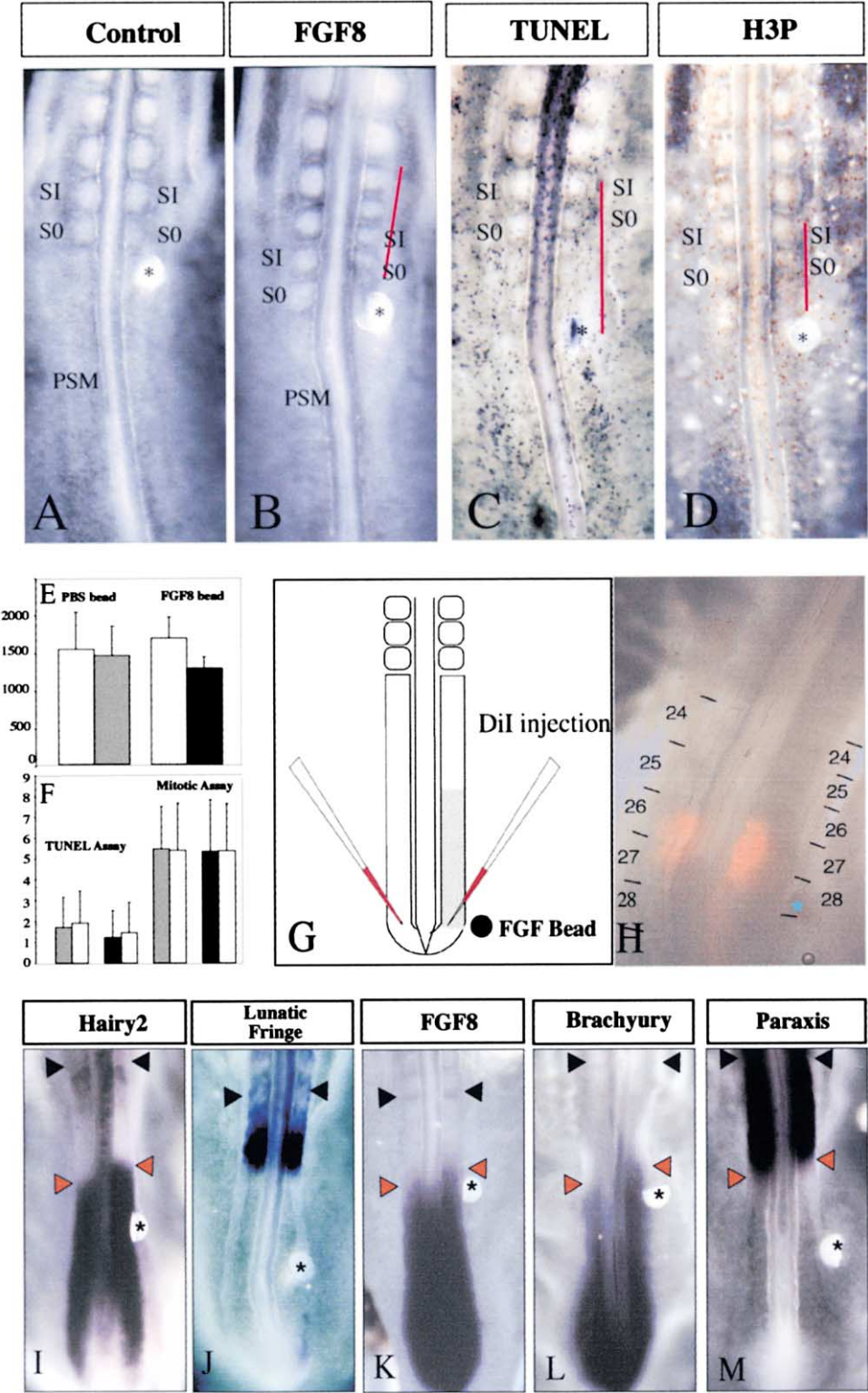
Figure 4. Implantation of an FGF8 Bead Reduces the Number of Cells Allocated to Somites

(A and B) 22-somite stage embryos fixed 12 hr after implantation of a PBS (A) or an FGF8 (B) bead (asterisk) in the caudal PSM. The red bar marks the region which forms smaller somites.

(C and D) FGF8 bead treated embryos fixed after 9 hr and processed by TUNEL to visualize apoptotic nuclei (in blue) (C) or by immunohistochemistry using the antibody against anti-phosphorylated histone H3 which labels the nuclei of dividing cells (in brown) (D). Apoptotic nuclei and proliferating cells were counted in the region between the bead and the forming somites when smaller somites start to form (red bar).

(E) Whereas the number of cells per somite is not significantly different between somites on the grafted (gray column) and control side

ligand diffusion model in which one would predict more severe abnormalities anterior to the bead (where the FGF8 gradient is steeper than normal) as opposed to posterior to the bead (where the gradient is less steep than normal). Another possiblity to account for this anisotropic effect is that given that FGF8 acts at the level of the determination front, an effect on territories located caudal to the bead could only occur when the bead is located in the rostral PSM. Because of the formation of a basal lamina containing laminin and fibronectin starting at the level of the determination front, the rostral PSM extracellular environment is very different from that of the caudal PSM (Duband et al., 1987). FGF8 which strongly binds heparan-sulfate, an important constituent of the extracellular matrix (Szebenyi and Fallon, 1999), might thus be limited in its diffusion in the rostral PSM and be unable to reach the level of the determination front.

Because FGF8 and FGF4 elicit similar biological responses in most assays examined thus far, we tested the specificity of the effect of FGF8 on segmentation by grafting FGF4 beads lateral to the caudal PSM. FGF4 beads caused a symmetric short-range disruption in the rostro-caudal organization of the somites located immediately adjacent to the bead (Figure 3G; n = 5/8). This suggests that either FGF8 differs greatly from FGF4 in its diffusion properties, or that a different relay mechanism is at work. We also compared the effect of FGF8 to that of the TGFβ family factor BMP4 in similar experimental conditions. Grafting a bead soaked in BMP4 revealed that it acts over a distance similar to that seen with FGF8 beads by downregulating *paraxis*. However, unlike FGF8, this effect is seen over the same distance anterior and posterior to the bead.

Taken together, these results indicate that a source of FGF8 provided caudally can modify the size of somites by acting at the level of the determination front in the PSM.

FGF8 Alters the Position of Somitic Boundaries and Reduces the Number of Cells Allocated to Each Somite

The formation of smaller somites induced by the graft of FGF8 beads could result either from a compaction of the cells in the affected somites if the number of cells per somite is not changed, or from a reduction in the number of cells allocated to each somite. To distinguish between these two possiblities, we counted the number of cells in the small somites induced by FGF8 bead grafts (Figures 4B and 4E). In the small somites, a reduction in

cell number ranging from 17% to 33% was observed when compared to the normal contralateral control somites (n = 3). No differences in cell counts were observed in somites of control embryos grafted with a bead soaked in PBS (Figures 4A and 4E, n = 2).

This difference in cell number might be accounted for by an increase in cell death induced by FGF8 in the region rostral to the bead. However, when apoptotic cells were counted in this region, in embryos harvested after less than 9 hr reincubation time, no significant increase in cell death was observed as compared with the contralateral side (Figures 4C and 4F, n = 3). A second possible cause for the observed reduction in cell number could be reduced cell proliferation. We assayed cell proliferation with an antibody against phosphorylated histone H3 to visualize dividing cells in embryos grafted with an FGF8 bead (Figures 4D and 4F; n = 3). A comparison of the number of labeled cells in the control and experimental regions rostral to the bead in embryos reincubated for up to 9 hr revealed no significant differences in cell proliferation. Similar counts performed in embryos grafted with control beads showed no differences in the number of proliferating (n = 2) and apoptotic (n = 2) cells between the two sides (Figure 4F).

We examined whether FGF8 would diminish the number of cells in the region rostral to the bead by inducing a caudal migration of PSM cells out of this area. To test this hypothesis, we labeled groups of mesodermal cells located in the most caudal part of the PSM with DiI at the same axial level on both sides of the embryo (Figure 4G). An FGF8 bead was then implanted caudal to one of these labeled groups and the embryo was incubated until the labeled cells were incorporated into somites. In all cases (n = 15), labeled cells remained at the same axial level on both sides of the embryo, whereas shifts in somite boundaries were observed in the region of labeled cells (Figure 4H). In the region closest to the grafted bead, where offsetting of the somitic boundaries was maximum, DiI-labeled cells are incorporated into differently numbered somites. These experiments therefore indicate that FGF8 reduces the number of cells allocated to each somite without increasing cell death or diminishing cell proliferation and without causing major cell rearrangements. Thus, the formation of smaller somites in response to FGF8 bead grafts is caused by changing the position of somitic boundaries while the absolute position of cells along the AP axis is not modified. This indicates that FGF signaling controls the positioning of somitic boundaries.

(white column) in control embryos (p > 0.5), a significant reduction in the number of cells was observed between the somites of the FGF8 bead-grafted side (black column) compared to control side (white column) (p < 0.0001).

(F) Average number of apoptotic and proliferating cells per section in PBS (gray columns) and FGF8 (black columns) treated sides compared to the contralateral side (white columns). Neither PBS nor FGF8 bead grafts increased apoptosis (p = 0.16 and p = 0.04, respectively) or cell proliferation (p > 0.5 in both cases) on the grafted side.

(G) Schematic representation of DiI labeling of caudal PSM cells before implantation of an FGF8 bead. (H) Distribution of labeled cells in an HH 18 stage embryo operated as described in (G) after 18 hr of incubation. (asterisk: grafted FGF8 bead).

(I–M) Whole-mount in situ hybridizations of HH14 stage embryos 5 to 8 hr following implantation of an FGF8 bead (asterisks) in the caudalmost part of the PSM. *c-hairy2* showing a phase I of the clock cycle (I). *Lunatic Fringe* showing a phase III of the clock cycle (J). *FGF8* (K). *Brachyury* (L). *paraxis* (M). Black arrowheads mark the rostral limit of the PSM. Red arrowheads point to the limit of expression of the different genes in the PSM.

Dorsal views, rostral to the top.

**FGF8 Does Not Accelerate the Segmentation Clock
but Shifts Rostrally the Determination Front**
The shift of the somitic boundaries in the grafted em-
bryos could result from an acceleration of the pace of
the segmentation clock. However, operated embryos in
which extrasomitic boundaries had formed on one side
but not on the other were never seen, suggesting that
the smaller somites on the operated side form at the
same pace as those of the control side. To determine
whether FGF8 acts on the pace of the segmentation
clock, we performed in situ hybridization on grafted em-
bryos with the cycling genes *c-hairy2* (n = 5) and *Lunatic
Fringe* (n = 24) (Figures 4I and 4J).

Expression patterns of the cycling genes have been
classified into three phases corresponding to the pro-
gression of the wave of expression along the PSM (Pal-
meirim et al., 1997). In phase I, the genes are expressed
in a broad caudal domain extending up to the level of
somite −IV (Figure 4I). In phases II and III, the cyclic
genes are expressed in the rostral PSM (Figure 4J). In
embryos grafted with an FGF8 bead and examined dur-
ing the determination of the smaller somites, the two
embryonic sides were always found to be in the same
phase of the clock cycle indicating that FGF8 does not
modify the period of the oscillation of the cycling genes
(Figures 4I and 4J).

However, an examination of grafted embryos which
were in phase I of the clock cycle reveals a rostral exten-
sion of the caudal expression domain on the grafted
side (Figure 4I). This observation suggests that ectopic
FGF8 induces a rostral extension of the undetermined
region. To further characterize this effect, in situ hybrid-
izations were performed on grafted embryos with mark-
ers associated with either the rostral determined region,
such as *paraxis* (n = 8) or with the caudal undetermined
region such as *FGF8* (n = 10) and *Brachyury* (n = 6). A
rostral extension of the expression domains of both
FGF8 and *Brachyury* and a rostral shift of the *paraxis*
expression domain were observed (Figures 4K–4M).
This ectopic activation of *FGF8* by FGF8 bead grafts
indicates an autocrine regulation of this gene in the
PSM. This autocrine effect might either act as a relay
for FGF8 or could amplify its diffusion, thus accounting
for the long-range action of FGF8. FGF8 also induces
Brachyury expression in the PSM, further suggesting the
existence of a loop linking *Brachyury* to FGF signaling
similar to that identified during amphibian gastrulation
(Schulte-Merker and Smith, 1995). Altogether, these re-
sults suggest that FGF8 can shift the determination front
rostrally in the PSM, thus delaying the segmental deter-
mination of caudal PSM cells.

**Blocking FGF Signaling Results in Larger
Somite Formation**
To further investigate the role of FGF signaling in the
regulation of segmentation, we blocked this pathway by
treating embryos in ovo with SU5402, a drug known to
specifically block the kinase activity of FGF receptors
(Mohammadi et al., 1997). In SU5402-treated embryos,
a large pair of somites was formed bilaterally by cells
that were located at the level of S-IV, at the time of the

injection (n = 12/19, Figures 5A and 5B). The number
of cells in such larger somites was counted on both sides
of an embryo and compared to that found in somites of
an equivalent axial level of a stage-matched control em-
bryo treated with DMSO only. The mean number of cells
per somite was 1554 cells for the control embryo and
1916 cells in the SU-treated embryo. The number of
cells of the enlarged somites was also found to be signifi-
cantly higher than that of the somite found immediately
rostral in the same embryos (n = 3, see Experimental
Procedures and Figure 5C).

To better characterize the effect of SU5402 treatment
on the PSM, we compared the effect of blocking FGF
signaling in half-embryos cultured in medium containing
SU5402 for the same time period as the control contra-
lateral half. We compared the expression of markers for
the rostral and caudal PSM domains, namely *paraxis* (n =
6), *FGF8* (n = 5), and *Brachyury* (n = 3), in the cultured
half-embryos (Figures 5D and 5F and data not shown).
The rostral boundary of the *FGF8* and *Brachyury* expres-
sion domains were shifted more caudally in drug-treated
half-embryos, suggesting that the determination front
was displaced caudally. In contrast, the caudal bound-
ary of the *paraxis* domain was not affected. We also
examined the expression of the cycling genes *c-hairy2*
(n = 8) and *Lunatic Fringe* (n = 3) and observed no phase
differences in the treated and control halves (Figure 5E
and data not shown). However, the rostral boundary of
the phase I expression domain was shifted caudally
(Figure 5E). Thus SU5402 acts at the determination front
level by inducing a caudal shift of somite boundaries
resulting in formation of larger somites.

**FGF8 Treatment Shifts Somitic *Hox* Gene
Boundaries Anteriorly**
During the production of smaller somites following the
graft of an FGF8 bead, the PSM becomes extended
rostrally by a length of up to one somite on the operated
side (compare the position of S0 on the two sides in
Figure 4B). Our DiI labeling experiments demonstrate
that cells of the same axial level will be incorporated
into differently numbered somites in the control and the
experimental side (Figure 4H). Given that the formation
of each somite is associated with one oscillation of the
cycling genes in the PSM, the cells of the region rostral
to the bead which become incorporated into a differently
numbered somite than their contralateral control cells
must therefore undergo an extra oscillation when com-
pared to these control cells. Evidence for such a super-
numerary oscillation is illustrated by the rostral exten-
sion of the phase I expression domains of *c-hairy2* and
Lunatic Fringe in the cells located rostral to the bead
(Figure 4I and data not shown).

What is the outcome of this extra oscillation on the
axial identity of these cells? To address this question,
we examined the formation of anterior *Hox* gene bound-
aries in FGF8-treated embryos. When an FGF8 bead is
grafted adjacent to the caudal PSM of 15- to 20-somite
stage embryos, the bead is usually found to lie in the
region adjacent to somites 25 to 30. Since up to 6–7
somites rostral to the grafted bead exhibit shifted
boundaries, the affected region lies between somites
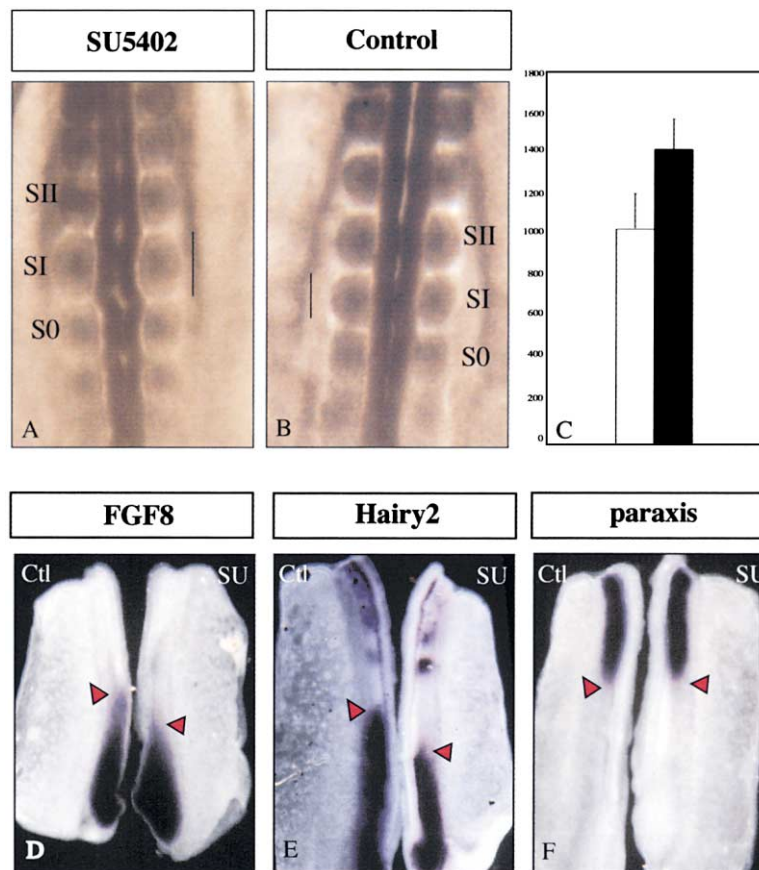20 to 30. We analyzed the expression of two *Hox* genes

Figure 5. SU5402 Increases the Number of Cells Allocated to a Somite and Shifts Caudally the Determination Front

(A and B) Dorsal views of HH13-14 stage embryos treated with SU5402 (A) or DMSO (B) and fixed after 10 hr of incubation. (A) 22-somite stage embryo treated with SU5402 at the 16-somite stage. The SI somite pair (somites 21) is enlarged compared to a stage-matched embryo treated with DMSO alone (B).

(C) Comparison of the number of cells per somite in the enlarged somites compared to unaffected somites (see Experimental Procedures). The number of cells is significantly increased in the affected somites (p = 0.0003).

(D–F) Whole-mount in situ hybridizations with *FGF8* (D), *c-hairy2* (E) and *paraxis* (F) on half-embryos cocultured for 80 to 100 min in presence of SU5402 (SU) or DMSO (Ctl).

which exhibit a rostral somitic boundary of expression in this region, namely *HoxB9* (n = 29) and *HoxA10* (n = 15), which have anterior boundaries at the level of somites 22/23 and 25/26, respectively (Burke et al., 1995; Cohn et al., 1997). In manipulated embryos displaying shifted somitic boundaries in a region including the anterior boundary of *HoxB9* or *HoxA10*, the anterior boundary of these genes was always shifted anteriorly so as to maintain a rostral limit at the correct somite number on the grafted side (Figures 6B and 6D). In contrast, when the position of the grafted bead was such that the affected region did not include the anterior boundary of expression of these genes, no such anterior shift of their expression limit was observed (not shown).

Since no cell movement along the AP axis of the PSM is observed upon FGF8 treatment, these results indicate that cells of the undetermined caudal region of the PSM can activate ectopic expression of genes like *HoxB9* or *HoxA10* in order to maintain the anterior limit of expression of these *Hox* genes at the appropriate somitic level. This ectopic activation of *Hox* genes indicates that the axial identity of cells in the caudal region of the PSM is not determined. Ectopic activation of *Hox* genes is only observed in cells which have undergone a supernumerary oscillation cycle, strongly suggesting a tight coupling between the segmentation clock and the spatiotemporal activation of *Hox* genes in the PSM.

Altering FGF signaling in frog and mouse embryos has been shown to have a profound effect on *Hox* gene expression along the body axis such that FGF signaling

can posteriorize the embryo (Pownall et al., 1996; Partanen et al., 1998). These data led to the idea that the level of FGF signaling is involved in defining axial identities along the body axis. However, close examination of our data demonstrating that FGF bead grafts can cause an ectopic activation of *Hox* genes indicates that this effect is not simply due to such a posteriorizing effect. First, none of the effects on segmentation that are observed can be explained by this type of posteriorizing effect. Second, if the level of FGF signaling specifies the AP identity of axial segments, the result of the bead graft experiment should be different depending on the AP level of the graft. A bead producing the same amount of FGF should elicit a stronger response when grafted in the caudal PSM at an earlier developmental stage (where lower FGF signaling is required) when compared to a bead grafted in a similar location at a later stage (where higher FGF signaling is required). Our data show that the same response is seen when beads loaded with the same amount of FGF are grafted in the caudal PSM at different developmental stages (Figure 6). In all cases these grafts resulted in smaller somite formation and a rostral extension of the *Hox* expression domain on the grafted side so as to maintain the anterior boundary at the appropriately numbered somite. Therefore, whereas a posteriorizing role of FGF signaling is likely to take place during gastrulation when paraxial mesoderm cells are produced (Pownall et al., 1996; Partanen et al., 1998), our results point to a different role for FGF signaling in coordinating the positioning of somitic boundaries with
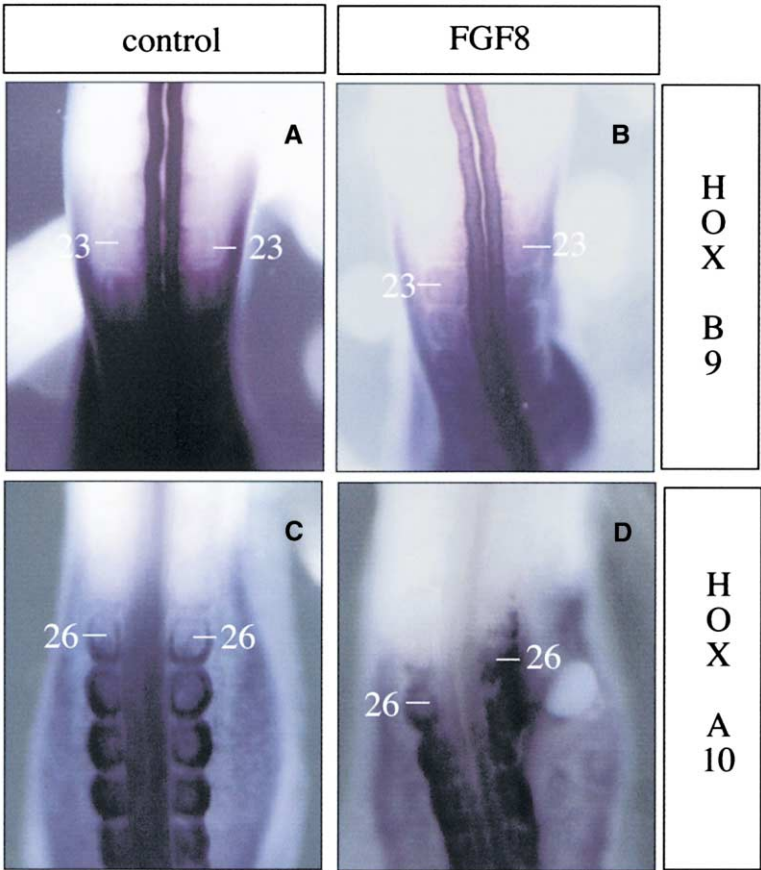
Figure 6. *Hox* Genes Activation in the Paraxial Mesoderm Is Coupled to the Segmentation Clock

Whole-mount in situ hybridization of HH stage 17–18 embryos with *HoxB9* (A and B) and *HoxA10* (C and D) in control (A and C) and FGF8-treated embryos (B and D). Dorsal views, anterior to the top.

Hox gene activation during later paraxial mesoderm development.

Conclusion

FGF Signaling Positions Segmental Boundaries

Our results demonstrate that the segmentation program and the axial identity of PSM cells is determined around the level of somite −IV. Caudal to this level, both the segmental schedule and combinatorial expression of *Hox* genes can be altered experimentally. We therefore term this level the "determination front" of the PSM. Our data demonstrate that *FGF8,* which is strongly expressed in the caudal-most PSM and then in a graded fashion up to the level of the determination front, plays an important role in maintaining cells of the caudal PSM undetermined and thus in positioning the determination front. Furthermore, by altering FGF signaling in the PSM, we show that this pathway acts at the level of the determination front to control the positioning of segmental boundaries.

We propose a model in which the future somite boundaries are periodically specified by the segmentation clock at the determination front level (Figure 7A). A movie presenting this model is available as supplemental data to this article (at http://www.cell.com/cgi/content/full/106/2/219/DC1). Our experiments suggest that the determination front represents the site at which FGF8 concentration drops below a critical threshold, thereby permitting segmental determination of prospective somites (Figure 7A). As the embryo extends posteriorly, the position of the determination front recedes along the anteroposterior axis while keeping its relative position in the PSM constant. A model in which cells endowed with boundary properties are periodically specified by the clock could explain how the flow of cells which pass through the determination front becomes allocated to defined somites. In particular, PSM cells would become competent for segmentation when FGF8 levels drop below a certain threshold (black line, Figure 7A), and adopt a boundary fate (blue) if they are juxtaposed to cells in a different phase of the segmentation cycle (in black, Figure 7A). Due to the oscillating nature of the cycling genes, this interface is transient, and so a small group of boundary cells are generated once per 90 min cycle. This model does not imply that formation of the boundaries actually occurs at the determination front level but that the boundary would be specified at this level and only forms at the rostral level of the PSM. Alternatively such a mechanism could also create an interface between cells allocated to future consecutive somites which could subsequently be transformed into a segmental boundary.

Grafting an FGF8 bead does not alter the pace of the clock but displaces rostrally the determination front (Figure 7B, magenta line). Thus, boundary specification will occur more rostrally in the PSM resulting in less cells being allocated to the prospective somite anterior to the boundary. Conversely, when FGF signaling is blocked by SU5402, there is still no effect on the period
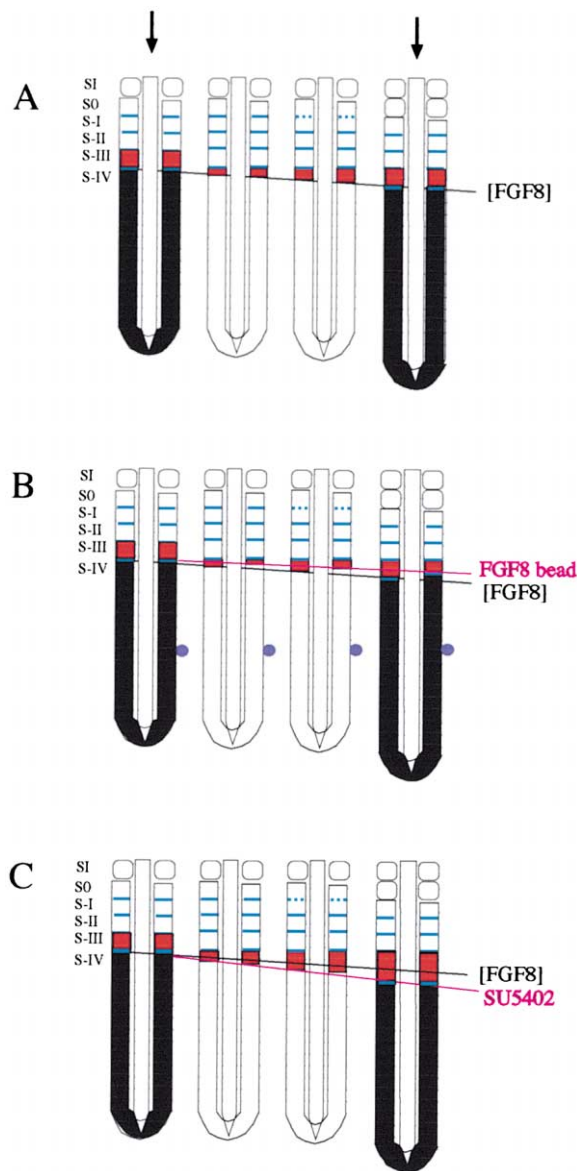
Figure 7. A Model for Segmental Determination Involving a Clock-Regulated Specification of Boundaries Controlled by FGF Signaling in the Chick PSM

(A–C) Schematic representation of segment determination during one oscillation of the segmentation clock in the normal situation (A), after implantation of an FGF8 bead (B), or after SU5402 treatment (C).

of oscillation of the cyclic genes, but the determination front is displaced caudally (Figure 7C, magenta line). The boundary will thus be positioned more caudally, leading to the formation of larger somites containing more cells than control somites.

This model is conceptually similar to the "clock and wavefront" model (Cooke and Zeeman, 1976; Jiang et al., 1998). In this model, PSM cells oscillate between different cellular states in response to a cellular oscillator or clock. The production of segmental boundaries occurs when cells in a permissive phase of the clock cycle encounter a maturation wavefront progressing caudally

in the PSM. As a result, segments are formed in a rostral-to-caudal fashion at a temporal frequency defined by the clock, and a spacing defined by the speed of wavefront progression in the PSM. The periodic expression of the cyclic genes has provided evidence for the existence of such a clock (Palmeirim et al., 1997). In addition, our results indicating that segmental boundaries are actually determined at the level of the determination front suggest that this level marks the true position of the wavefront in the PSM.

In the clock and wavefront model, somite size is a function of the period of the clock and of the speed of wavefront progression in the PSM. Production of smaller somites can be acheived either by accelerating the clock while the speed of the wavefront is kept constant or by slowing down the progression of the wavefront while keeping the period of the clock oscillations constant. Our results do not resemble an example of the first possibility because (1) whereas speeding the clock on the bead-grafted side would lead to asynchrony in the timing of boundary formation, somitic boundaries always form in synchrony between the control and grafted sides; and (2) the period of oscillation of the cycling genes is not affected by the bead graft.

In contrast, our observations do seem to represent an example of the second possibility. Normally, the relative position of the wavefront in the PSM is maintained at a constant level because its absolute position along the AP axis is constantly receding at the speed of somitogenesis during caudal embryo extension. Slowing down the wavefront while the speed of the caudal extension of the embryo is not changed will result in the relative position of the wavefront in the PSM becoming progressively displaced rostrally. In embryos grafted with an FGF bead, we observed that the determination front is shifted rostrally in the PSM in comparison to the control side. Thus, whereas FGF bead grafts do not modify the period of the clock oscillation, their effect can be interpreted as slowing down wavefront progression in the PSM, assuming that the wavefront corresponds to the determination front. A similar explanation could apply to the SU5402 inhibitor treatment which does not affect the period of the clock but would speed up the progression of the wavefront. In light of our data, this model thus offers an explanation for how clock oscillations are translated into the periodic array of somite boundaries.

Coupling Temporal Colinearity to the Segmentation Clock

How the spatiotemporal, or temporal colinearity, of *Hox* gene activation is implemented during development remains unclear. It has been proposed that the *Hox* complexes are initially in a closed configuration preventing transcription of these genes and that the complexes become progressively opened during development. This opening of the complexes would sequentially release the genes from a repressive influence rendering them progressively available to transcription (Kondo and Duboule, 1999). The timing mechanism which controls the stepwise opening of the complexes and which thus ensures that a given gene will be activated at the appropriate axial level is unknown. In the limb, proliferation of cells in the progress zone was proposed to act as

such a timing mechanism controlling the progressive opening of the *HoxD* cluster (Duboule, 1995).

Such a model could be applied to the paraxial mesoderm in which the opening of the *Hox* clusters could be linked to the number of cell divisions experienced by the stem cells in the primitive streak and tail bud from which the tissue originates (Dale and Pourquié, 2000; Nicolas et al., 1996; Stern et al., 1992). In this case, the opened configuration of the *Hox* clusters reached by descendants of the stem cells would be frozen upon their entering in the PSM. The fact that activation of *Hox* gene expression is seen in the caudal PSM is in agreement with this hypothesis (Gaunt and Strachan, 1996).

Our experiments indicate that PSM cells only become irreversibly determined with respect to their axial identity later, at the level of the determination front. This apparent plasticity of caudal PSM cells is thus in contradiction with a strict interpretation of the model whereby *Hox* gene expression is fixed on entry to the PSM. Rather, our results favor a two-step mechanism responsible for assigning precise *Hox* gene combinatorial expression to somites. In a first step, the clusters would progressively acquire their opened configuration in precursors of the paraxial mesoderm prior to their entering the PSM, by a mechanism which could be linked to cell proliferation in the stem cells. In the second step, which would occur at the level of the determination front, the definitive expression of *Hox* genes would be allocated to each prospective somite as it becomes determined. Our experiments suggest that this second phase is coupled to the segmentation clock, since increasing the number of oscillations in the PSM cells results in a posteriorization of these cells. The recent demonstration of a dynamic expression of *Hox* genes in the rostral mouse PSM further argue for a control of *Hox* gene activation by the segmentation clock (Zákány et al., 2001 [this issue of *Cell*]). Such a mechanism could explain how individual somites acquire their regional identity.

Experimental Procedures

Embryos and Nomenclature
Fertilized chick eggs were obtained from commercial sources. Eggs were incubated at 38°C in a humidified incubator and embryos were staged according to the developmental table of Hamburger and Hamilton (HH) (1992) and by counting somite pairs.

The forming somite, in which the caudal border is not completely formed, is referred to as somite 0. The remaining PSM tissue is divided into units of one somite in length (100–150 μm) as measured by a lens reticle. Each unit is identified by a negative roman number with respect to its position along the AP axis in reference to somite 0 (Figure 1A). Usually 12 to 14 units are present in the PSM. We refer to these units as "presumptive somites."

Surgery: Inversions of Presumptive Somites
Inversions of PSM fragments were performed in ovo. The ectoderm overlying the PSM was peeled back using tungsten needles. The region of interest was delimited by transverse and parasagittal incisions through the mesoderm, isolated, and immediately replaced in an inverted AP orientation. Small amounts of pancreatin (GIBCO) were added to facilitate the dissection. The ends of the inverted tissue were marked with carbon particles. After the operation, embryos were allowed to develop for 3 to 24 hr, until the grafted tissue had segmented. Embryos were then fixed and hybridized with the *delta1* probe.

Bead Implantation
Heparin beads (Sigma) were extensively washed in PBS and soaked overnight at 4°C in PBS, 1% BSA containing either FGF8b (1 mg/ml) or FGF4 (400 μg/ml) (R&D Systems). The FGF4 concentration was chosen because of its increased activity in a mitogenic assay on quiescent NR6R-3T3 when compared to FGF8 (ED50 = 0.15 ng/ml and 1 ng/ml for FGF4 and FGF8b, respectively). For BMP4 (200 μg/ml) (R&D Systems) affiblue-gel beads (BioRad) were treated in a similar fashion. 100–150 μm diameter beads were selected, cut in two equal parts and rinsed in a drop of PBS before implantation into 12- to 20-somite stage chick embryos. An incision through the ectoderm and the mesoderm was made to insert the bead between the paraxial and lateral mesoderm. Control beads soaked in PBS were grafted in similar manner. Embryos were incubated for 3 to 24 hr, and were then fixed for further analysis.

Plasmids and In Situ Hybridizations
Whole-mount in situ hybridizations were performed as described in Henrique et al. (1995). The chick *Brachyury, MyoD, pax3, c-hairy2, delta1, Lunatic Fringe, FGF8, FGFR1, paraxis, HoxB9*, and *HoxA10* have been described (Burke et al., 1995; Goulding et al., 1994; Henrique et al., 1995; Hirsinger et al., 2001; Jouve et al., 2000; Knezevic et al., 1997; McGrew et al., 1998; Patstone et al., 1993; Sosic et al., 1997; Vogel et al., 1996). Plasmid DNA for electroporations was purified using an endotoxin-free maxi kit (Quiagen) and resuspended in PBS. The GFP expression vector contains the coding sequence for a destabilized eGFP (d1EGFP, Clontech) subcloned into the pCAAGS expression vector (Niwa et al., 1991). The pMIW cFGF8b expression vector was described in Araki and Nakamura (1999). A solution of PBS, 1 mM MgCl₂, 0.4 mg/ml fast green FCF (Sigma) containing 1 μg/μl of GFP vector and either 1.5 μg/μl of FGF8 vector or the empty pCAAGS vector was used for electroporations.

In Ovo Electroporation
Embryos of stage 4–5 HH were used for electroporations. Eggs were windowed and the DNA solution was injected between the vitelline membrane and the epiblast. The primitive streak was coated with the DNA solution from the node until mid-streak. A 4.0 mm long gold-tipped electrode (0.4 mm diameter, TR Tech) was placed directly on the streak caudal to the node. A second 3.0 mm long tungsten wire (0.4 mm diameter) was inserted into the yolk under the gold-tipped electrode. A series of electric pulses (3–6 pulses, 80 volts, 40 ms) were directed toward the tungsten electrode using a square wave electroporator (BTX T820). Eggs were reincubated for 24 hr and assayed for GFP expression. Embryos displaying a normal overt morphology and positive for GFP expression in the PSM (10%–50%) were processed for subsequent analysis.

Immunohistochemistry and TUNEL Assay
An antibody raised against phosporylated Histone H3 (Upstate Biotechnology) was used to analyze cell proliferation. Operated embryos were fixed in 4% paraformaldehyde, dehydrated through a graded methanol solution series and processed in whole mount as described in Stern (1998). Anti-Histone H3 primary antibody was used at 1/1000 and anti-rabbit IgG coupled to HRP (Jackson labs) was used to 1/100. Apoptosis was assayed by TUNEL (Apoptag kit, Oncor) on whole-mount embryos as described in Yamamoto and Henderson (1999).

DiI Labeling
DiI crystals (Molecular Probes) were dissolved in ethanol to a final concentration of 1 mg/ml. After removal of the overlying ectoderm, small groups of PSM cells were labeled at the same axial level on both sides of the embryo by pressure injection using a Picospritzer II injector with micropipettes (~5 μm of diameter). Dye applications were performed under a Leica MZFLIII stereomicroscope equipped with rhodamine fluorescent filters. After labeling, embryos which had received focal injections at exactly equivalent AP positions were selected and implanted with an FGF8b bead in the vicinity of one group of labeled cells. These embryos were reincubated until the region adjacent to the bead was fully segmented.

SU5402 In Ovo Treatment and Half Embryo Assay

SU5402 (Calbiochem; Mohammadi et al., 1997) was used to block FGF signaling in ovo. A SU5402 stock solution in DMSO was diluted in PBS/ATP (1 mM) to a final concentration of 400 μM in 0.5% DMSO. The number of somites was counted and 50 μl of the PBS/ATP/SU5402 solution was directly added onto the caudal part of the embryos which were reincubated for 45 min to an hour and then thoroughly washed with PBS. Embryos were then reincubated for 10 hr. Control embryos were treated similarly with a 0.5% DMSO solution. Embryos were fixed and processed for in situ hybridization (not shown) or for cell counting.

Half-embryo cultures were performed as described in Palmeirim et al. (1997). One half was cultured in medium containing 80 μM SU5402 whereas the control half was cultured in DMSO containing medium. Both halves were cultured for 80 to 100 min and fixed for in situ hybridization.

Quantitative Analyses

To assess the total number of cells per somite after FGF8 bead or SU5402 treatment, embryos were fixed in Carnoy's fluid, dehydrated in ethanol, and rehydrated in PBS, 0.1% Tween 20 (PBT). Ectoderm was removed from the region of interest, and the embryos were stained overnight at room temperature using the Oligreen DNA marker to label cell nuclei (Molecular Probes, 1/2000 in PBT). After extensive washes, embryos were flat-mounted in 20% glycerol. Nuclei of somitic cells were counted using a Zeiss confocal microscope. Coronal sections were acquired every 7 μm from the dorsal to the ventral surface of the somite. Nuclei in each of the resulting sections were counted and summed.

Cell number in somites of embryos grafted with FGF8 (n = 3) or PBS (n = 2) beads were compared with the contralateral somites. The mean number of cells ± SEM is presented for each condition in Figure 4E.

Cell number in somites (SI, n = 2 experimental somites) of a SU5402-treated embryo was directly compared to the cell number of equivalent somites (SI, n = 2 control somites) of a staged-matched DMSO-treated embryo. In addition, in three 12- to 16-somite stage embryos, the number of cells was counted in the large somites (n = 6 experimental somites) and compared to the cell number in the somites located immediately rostrally in the same embryos (n = 6 control somites). Counts of control somites (n = 8) and experimental somites (n = 8) were separately summed and divided by the number of counted somites. Results are presented in Figure 5C as means ± SEM.

The number of mitotic and apoptotic cells in bead-implanted embryos were quantified after Histone H3 and TUNEL labeling. Whole-mount stained embryos were paraffin-embedded and serially sectioned (7.0 μm) using a microtome. A minimum of 50 consecutive sections were analyzed per embryo from the implanted bead rostral-ward (Figures 4C and 4D, red bar). Given the low number of positive nuclei on each section (0 to 10), we could directly verify the absence of significant nuclear overlap between sections. Mean number ± SEM of positive nuclei per section was compared between the grafted and control sides of the embryos and is shown in Figure 4F. P values for all cell counts are determined by two-tailed paired t tests.

References

Aoyama, H., and Asamoto, K. (1988). Determination of somite cells: independence of cell differentiation and morphogenesis. Development *104*, 15–28.

Araki, I., and Nakamura, H. (1999). Engrailed defines the position of dorsal di-mesencephalic boundary by repressing diencephalic fate. Development *126*, 5127–5135.

Burgess, R., Cserjesi, P., Ligon, K.L., and Olson, E.N. (1995). Paraxis: a basic helix-loop-helix protein expressed in paraxial mesoderm and developing somites. Dev. Biol. *168*, 296–306.

Burke, A.C., Nelson, C.E., Morgan, B.A., and Tabin, C. (1995). Hox genes and the evolution of vertebrate axial morphology. Development *121*, 333–346.

Cohn, M.J., Patel, K., Krumlauf, R., Wilkinson, D.G., Clarke, J.D., and Tickle, C. (1997). Hox9 genes and vertebrate limb specification. Nature *387*, 97–101.

Cooke, J., and Zeeman, E.C. (1976). A clock and wavefront model for control of the number of repeated structures during animal morphogenesis. J. Theor. Biol. *58*, 455–476.

Crossley, P.H., and Martin, G.R. (1995). The mouse Fgf8 gene encodes a family of polypeptides and is expressed in regions that direct outgrowth and patterning in the developing embryo. Development *121*, 439–451.

Dale, K.J., and Pourquié, O. (2000). A clock-work somite. Bioessays *22*, 72–83.

Deuchar, E., and Burgess, A.M.C. (1967). Somite segmentation in amphibian embryos: is there a transmitted control mechanism? J. Embryol. Exp. Morphol. *17*, 349–358.

Duband, J.L., Dufour, S., Hatta, K., Takeichi, M., Edelman, G.M., and Thiery, J.P. (1987). Adhesion molecules during somitogenesis in the avian embryo. J. Cell Biol. *104*, 1361–1374.

Duboule, D. (1995). Vertebrate Hox genes and proliferation: an alternative pathway to homeosis? Curr. Opin. Genet. Dev. *5*, 525–528.

Gaunt, S.J., and Strachan, L. (1996). Temporal colinearity in expression of anterior Hox genes in developing chick embryos. Dev. Dyn. *207*, 270–280.

Goulding, M., Lumsden, A., and Paquette, A.J. (1994). Regulation of Pax-3 expression in the dermomyotome and its role in muscle development. Development *120*, 957–971.

Henrique, D., Adam, J., Myat, A., Chitnis, A., Lewis, J., and Ish-Horowicz, D. (1995). Expression of a Delta homologue in prospective neurons in the chick. Nature *375*, 787–790.

Hirsinger, E., Jouve, C., Dubrulle, J., and Pourquié, O. (2000). Somite formation and patterning. Int. Rev. Cytol. *198*, 1–65.

Hirsinger, E., Malapert, P., Dubrulle, J., Delfini, M.C., Duprez, D., Henrique, D., Ish-Horowicz, D., and Pourquié, O. (2001). Notch signalling acts in postmitotic avian myogenic cells to control MyoD activation. Development *128*, 107–116.

Jiang, Y.-J., Smithers, L., and Lewis, J. (1998). The clock is linked to notch signalling. Curr. Biol. *8*, R868–R871.

Jouve, C., Palmeirim, I., Henrique, D., Beckers, J., Gossler, A., Ish-Horowicz, D., and Pourquié, O. (2000). Notch signalling is required for cyclic expression of the hairy-like gene HES1 in the presomitic mesoderm. Development *127*, 1421–1429.

Kerszberg, M., and Wolpert, L. (2000). A clock and trail model for somite formation, specialization and polarization. J. Theor. Biol. *205*, 505–510.

Keynes, R.J., and Stern, C.D. (1988). Mechanisms of vertebrate segmentation. Development *103*, 413–429.

Kieny, M., Mauger, A., and Sengel, P. (1972). Early regionalization of somitic mesoderm as studied by the development of axial skeleton of the chick embryo. Dev. Biol. *28*, 142–161.

Knezevic, V., De Santo, R., and Mackem, S. (1997). Two novel chick T-box genes related to mouse Brachyury are expressed in different, non-overlapping mesodermal domains during gastrulation. Development *124*, 411–419.

Kondo, T., and Duboule, D. (1999). Breaking colinearity in the mouse HoxD complex. Cell *97*, 407–417.

McGrew, M.J., Dale, J.K., Fraboulet, S., and Pourquié, O. (1998). The lunatic fringe gene is a target of the molecular clock linked to somite segmentation in avian embryos. Curr. Biol. *8*, 979–982.

Meinhardt, H. (1986). Models of segmentation. In Somites in Developing Embryos, R. Bellairs, D.A. Ede, and J.W. Lash, eds. (New York: Plenum press), pp. 179–191.

Menkes, B., and Sandor, S. (1977). Somitogenesis, regulation potencies, sequence determination and primordial interactions. In Vertebrate Limb and Somite Morphogenesis. British Society Dev. Biol. Symposium *3*, D.A. Ede, D.A. Hinchcliffe, and M. Balls, eds. (Cambridge: Cambridge University Press), pp. 405–419.

Mohammadi, M., McMahon, G., Sun, L., Tang, C., Hirth, P., Yeh, B.K., Hubbard, S.R., and Schlessinger, J. (1997). Structures of the tyrosine kinase domain of fibroblast growth factor receptor in complex with inhibitors. Science *276*, 955–960.

Nicolas, J.F., Mathis, L., Bonnerot, C., and Saurin, W. (1996). Evidence in the mouse for self-renewing stem cells in the formation of a segmented longitudinal structure, the myotome. Development *122*, 2933–2946.

Niwa, H., Yamamura, K., and Miyazaki, J. (1991). Efficient selection for high-expression transfectants with a novel eukaryotic vector. Gene *108*, 193–199.

Nowicki, J.L., and Burke, A.C. (2000). Hox genes and morphological identity: axial versus lateral patterning in the vertebrate mesoderm. Development *127*, 4265–4275.

Packard, D.S.J. (1978). Chick somite determination: the role of factors in young somites and the segmental plate. J. Exp. Zool. *203*, 295–306.

Palmeirim, I., Henrique, D., Ish-Horowicz, D., and Pourquié, O. (1997). Avian hairy gene expression identifies a molecular clock linked to vertebrate segmentation and somitogenesis. Cell *91*, 639–648.

Palmeirim, I., Dubrulle, J., Henrique, D., Ish-Horowicz, D., and Pourquié, O. (1998). Uncoupling segmentation and somitogenesis in the chick presomitic mesoderm. Dev. Genet. *23*, 77–85.

Partanen, J., Schwartz, L., and Rossant, J. (1998). Opposite phenotypes of hypomorphic and Y766 phosphorylation site mutations reveal a function for Fgfr1 in anteroposterior patterning of mouse embryos. Genes Dev. *12*, 2332–2344.

Patstone, G., Pasquale, E.B., and Maher, P.A. (1993). Different members of the fibroblast growth factor receptor family are specific to distinct cell types in the developing chicken embryo. Dev. Biol. *155*, 107–123.

Pourquié, O. (2000). Vertebrate segmentation: is cycling the rule? Curr. Opin. Cell Biol. *12*, 747–751.

Pownall, M.E., Tucker, A.S., Slack, M.W., and Isaacs, H.W. (1996). eFGF, Xcad3 and Hox genes form a molecular pathway that establishes the anteroposterior axis in Xenopus. Development *122*, 3881–3892.

Schulte-Merker, S., and Smith, J.C. (1995). Mesoderm formation in response to Brachyury requires FGF signalling. Curr. Biol. *5*, 62–67.

Sosic, D., Brand-Saberi, B., Schmidt, C., Christ, B., and Olson, E.N. (1997). Regulation of paraxis expression and somite formation by ectoderm- and neural tube-derived signals. Dev. Biol. *185*, 229–243.

Stern, C.D. (1998). Detection of multiple gene products simultaneously by in situ hybridization and immunohistochemistry in whole mounts of avian embryos. Curr. Top. Dev. Biol. *36*, 223–243.

Stern, C.D., Fraser, S.E., Keynes, R.J., and Primmett, D.R. (1988). A cell lineage analysis of segmentation in the chick embryo. Development *104*, 231–244.

Stern, C.D., Hatada, Y., Selleck, M.A., and Storey, K.G. (1992). Relationships between mesoderm induction and the embryonic axes in chick and frog embryos. Dev. Suppl., 151–156.

Sun, X., Meyers, E.N., Lewandoski, M., and Martin, G.R. (1999). Targeted disruption of Fgf8 causes failure of cell migration in the gastrulating mouse embryo. Genes Dev. *13*, 1834–1846.

Szebenyi, G., and Fallon, J.F. (1999). Fibroblast growth factors as multifunctional signaling factors. Int. Rev. Cytol. *185*, 45–106.

Vogel, A., Rodriguez, C., and Izpisua-Belmonte, J.C. (1996). Involvement of FGF-8 in initiation, outgrowth and patterning of the vertebrate limb. Development *122*, 1737–1750.

Yamaguchi, T.P., Conlon, R.A., and Rossant, J. (1992). Expression of the fibroblast growth factor receptor FGFR-1/flg during gastrulation and segmentation in the mouse embryo. Dev. Biol. *152*, 75–88.

Yamaguchi, T.P., Harpal, K., Henkemeyer, M., and Rossant, J. (1994). fgfr-1 is required for embryonic growth and mesodermal patterning during mouse gastrulation. Genes Dev. *8*, 3032–3044.

Yamamoto, Y., and Henderson, C.E. (1999). Patterns of programmed cell death in populations of developing spinal motoneurons in chicken, mouse, and rat. Dev. Biol. *214*, 60–71.

Zákány, J., Kmita, M., Alarcon, P., de la Pompa, J.-L., and Duboule, D. (2001). Localized and transient transcription of *Hox* genes suggests a link between patterning and the segmentation clock. Cell *106*, this issue, 207–217.